TISSUE ENGINEERING: Part A
Volume 27, Numbers 5 and 6, 2021

DOI: 10.1089/ten.tea.2020.0052

termis
Tissue Engineering
& Regenerative Medicine
International Society

ORIGINAL ARTICLE

Predifferentiated Gingival Stem Cell-Induced Bone Regeneration in Rat Alveolar Bone Defect Model

Umadevi Kandalam, PhD,[1] Toshihisa Kawai, DDS, PhD,[1] Geeta Ravindran, PhD,[2,3]
Ross Brockman, DMD,[1,4] Jorge Romero, DMD,[1] Matthew Munro, DMD,[1] Julian Ortiz, DMD,[1]
Alireza Heidari, PhD,[1] Ron Thomas, BS,[2] Sajish Kuriakose, MDS, FFDRCSI,[5]
Christopher Naglieri, DMD,[1] Shaileen Ejtemai, DMD,[1] and Steven I. Kaltman, DMD, MD[1,6]

Cleft alveolus, a common birth defect of the maxillary bone, affects one in 700 live births every year. This defect is traditionally restored by autogenous bone grafts or allografts, which may possibly cause complications. Cell-based therapies using the mesenchymal stem cells (MSCs) derived from human gingiva (gingiva-derived mesenchymal stem cells [GMSCs]) is attracting the research interest due to their highly proliferative and multilineage differentiation capacity. Undifferentiated GMSCs expressed high level of MSC-distinctive surface antigens, including CD73, CD105, CD90, and CD166. Importantly, GMSCs induced with osteogenic medium for a week increased the surface markers of osteogenic phenotypes, such as CD10, CD92, and CD140b, indicating their osteogenic potential. The objective of this study was to assess the bone regenerative efficacy of predifferentiated GMSCs (dGMSCs) toward an osteogenic lineage in combination with a self-assembling hydrogel scaffold PuraMatrix™ (PM) and/or bone morphogenetic protein 2 (BMP2), on a rodent model of maxillary alveolar bone defect. A critical size maxillary alveolar defect of 7 mm × 1 mm × 1 mm was surgically created in athymic nude rats. The defect was filled with either PM/BMP2 or PM/dGMSCs or the combination of three (PM/dGMSCs/BMP2) and the bone regeneration was evaluated at 4 and 8 weeks postsurgery. New bone formation was evaluated by microcomputed tomography and histology using Hematoxylin and Eosin staining. The results demonstrated the absence of spontaneous bone healing, either at 4 or 8 weeks postsurgery in the defect group. However, the PM/dGMSCs/BMP2 group showed significant enhancement in bone regeneration at 4 and 8 weeks postsurgery, compared with the transplantation of individual material/cells alone. Apart from developing the smallest critical size defect, results showed that PM/dGMSCs/BMP2 could serve as a promising option for the regeneration of bone in the cranio/maxillofacial region in humans.

Keywords: cleft alveolus, human gingiva-derived mesenchymal stem cells, hydrogel, critical size defect, bone regeneration

Impact Statement

Gingiva-derived mesenchymal stem cells (GMSCs) are the most appealing cell source as they are readily accessible and capable of multilineage differentiation. They are most suitable for bone regeneration in craniofacial defects, due to their origin from neural crest progenitor cells. In this study, we have demonstrated that combination of predifferentiated osteogenic GMSCs (dGMSCs), self-assembling hydrogel, and low doses of BMP2 accelerated bone regeneration of alveolar bone defect in rat model suggesting that dGMSCs may lead to a novel cell therapy for enhanced bone regeneration in alveolar cleft and other bone defect complications in the craniofacial area.

[1]Department of Oral Sciences and Translational Research, College of Dental Medicine, Nova Southeastern University, Fort Lauderdale, Florida, USA.
[2]NSU Cell Therapy Institute, Dr. Kiran C. Patel College of Allopathic Medicine, Nova Southeastern University, Fort Lauderdale, Florida, USA.
[3]Department of Medicine, Karolinska Institutet, Stockholm, Sweden.
[4]Oral and Maxillofacial, LSU Health Sciences Center New Orleans, New Orleans, Louisiana, USA.
Departments of [5]Oral Medicine and Oral Surgery and [6]Oral and Maxillofacial Surgery, College of Dental Medicine, Nova Southeastern University, Fort Lauderdale, Florida, USA.

Introduction

Alveolar cleft is a common congenital malformation, with a worldwide incidence of ~1 in every 700–800 live births.[1] Maxillary alveolar clefts involve tooth-bearing bone of the upper jaw and are associated with dental anomalies, cosmetic anomalies owing to lack of support of alar base, and functional anomalies in speech, mastication, and swallowing because of the oronasal communication.

The repair of critical size craniofacial defects requires the gold standard autografts or allografts. However, the limitations involved in these procedures include, limited supply of grafts, risk of transmitting virus infection, or induction of immune rejection to the grafted allogeneic bone. Tissue-engineering strategies have emerged as a viable option for reconstruction of bone in large defects. For example, the approach of cell transplantation for alveolar bone reconstruction has utilized bone marrow-derived stem cells,[2–4] whereas other studies showed the successful outcomes from the implantation of adipose-derived stem cells and umbilical cord stem cells.[5–8]

Recently, orofacial-derived stem cells have gained attention in craniofacial bone reconstruction as they are highly proliferative and can be easily harvested using a minimally invasive method. The stem cells derived from dental pulp has been tested for bone regeneration in maxillary alveolar cleft.[9,10]

Mesenchymal stem cells (MSCs) obtained from human gingival connective tissue is rich in mesenchymal progenitor cells.[11] Especially, the gingiva-derived mesenchymal stem cells (GMSCs) are easily accessible cell source, and can be guided into osteogenic precursors.[12,13] Similar to other MSCs, GMSCs also possess an immune-privileged property with anti-inflammatory effect, making them excellent choices for autologous, as well as allogeneic, grafting.[14–18] Furthermore, studies have shown that 90% of GMSCs are derived from cranial neural crest cells[15] and thus superior in craniofacial bone regeneration to other MSCs, as they are programmed to participate in craniofacial development.[19]

This study aimed to investigate the efficacy of predifferentiated GMSCs (dGMSCs) in bone regeneration using a rat model of alveolar defect. Herein, we used an injectable self-assembling peptide, the hydrogel PuraMatrix™ (PM), as a carrier scaffold material for dGMSCs along with recombinant bone morphogenetic protein 2 (BMP2). BMP2 is a potent growth factor and plays an essential role in osteogenic induction.[20] It was hypothesized that low doses of BMP2 and dGMSCs formulated in a hydrogel that self-assembles *in situ* will secure the space for the injected dGMSCs and accelerate local differentiation of GMSCs to osteogenic progenitors.

Materials and Methods

Animals

A total of 30 athymic nude rats (8-week-old, male, body weight = 275–300 g, Hsd:RH-Foxn1rnu) purchased from Envigo (Indianapolis, IN) were acclimated to the vivarium at Nova Southeastern University (NSU) for a week, before starting the experiments. The study protocol used in this study was approved by the NSU Institutional Animal Care and Use Committee (IACUC Protocol # UK1 2017). Rats were divided into five groups: (1) control defect alone ($n = 6$), (2) PM alone ($n = 6$), (3) PM/dGMSCs ($n = 6$), (4) PM/BMP2 ($n = 6$), and (5) PM/dGMSCs/BMP2 ($n = 14$). Animals were housed in a light- and temperature-controlled environment and given food and water *ad libitum*.

Surgical protocol

The surgical procedures were performed on the anesthetized rats (Ketamine, 80–100 mg/kg and Xylazine 0.5–10 mg/kg) under sterile condition. The tongue was retracted anteriorly and laterally using a vicryl 3-0 suture (Henry Schein, Melville, NY). A 1.5 cm midcrestal incision was made just behind the upper incisor, leaving a cuff of soft tissue around the incisor. A full-thickness mucoperiosteal flap was elevated and then reflected buccally and palatally using a periosteal elevator. Using a #329 pear-shaped carbide bur (Brasseler, Savannah, GA) attached to a low-speed hand piece, a rectangular defect (7 mm × 1 mm × 1 mm) was created behind the incisor teeth on the lateral surface of the maxillary alveolar bone under constant irrigation with sterile saline. A similar defect was created on the other side. After the surgery, the mucoperiosteal flap was repositioned and sutured with two interrupted sutures using 4-0 Chromic Gut suture (Henry Schein) to achieve primary closure.

Postoperative care

The health status of animals was observed twice a day for 7 days after surgery, and then once daily for 2 weeks. Regular monitoring included signs of pain and discomfort of all rats (reduced activity, porphyrin staining, lethargy, loss

Table 1. Detailed Information of the Antibodies Used for Flow Cytometry Analysis

Antigen	*Conjugation*	*Company*	*Clone number*
CD73	APC-Cy7	BioLegend	AD2
CD90	FITC	BioLegend	5E10
CD105	BV711	BD Biosciences	266
CD166	PE-Cy7	BioLegend	3A6
CD45	BUV395	BD Biosciences	HI30
CD31	PE-Dazzle 594	BioLegend	WM59
CD34	PE	BD Biosciences	581
CD14	BUV805	BD Biosciences	M5E2
HLA DR	PerCP-Cy 5.5	BD Biosciences	G46–6
CD10	FITC	BioLegend	HI10a
CD140b	APC	R&D Systems	PR7212
CD92	PE	BioLegend	VIM15b

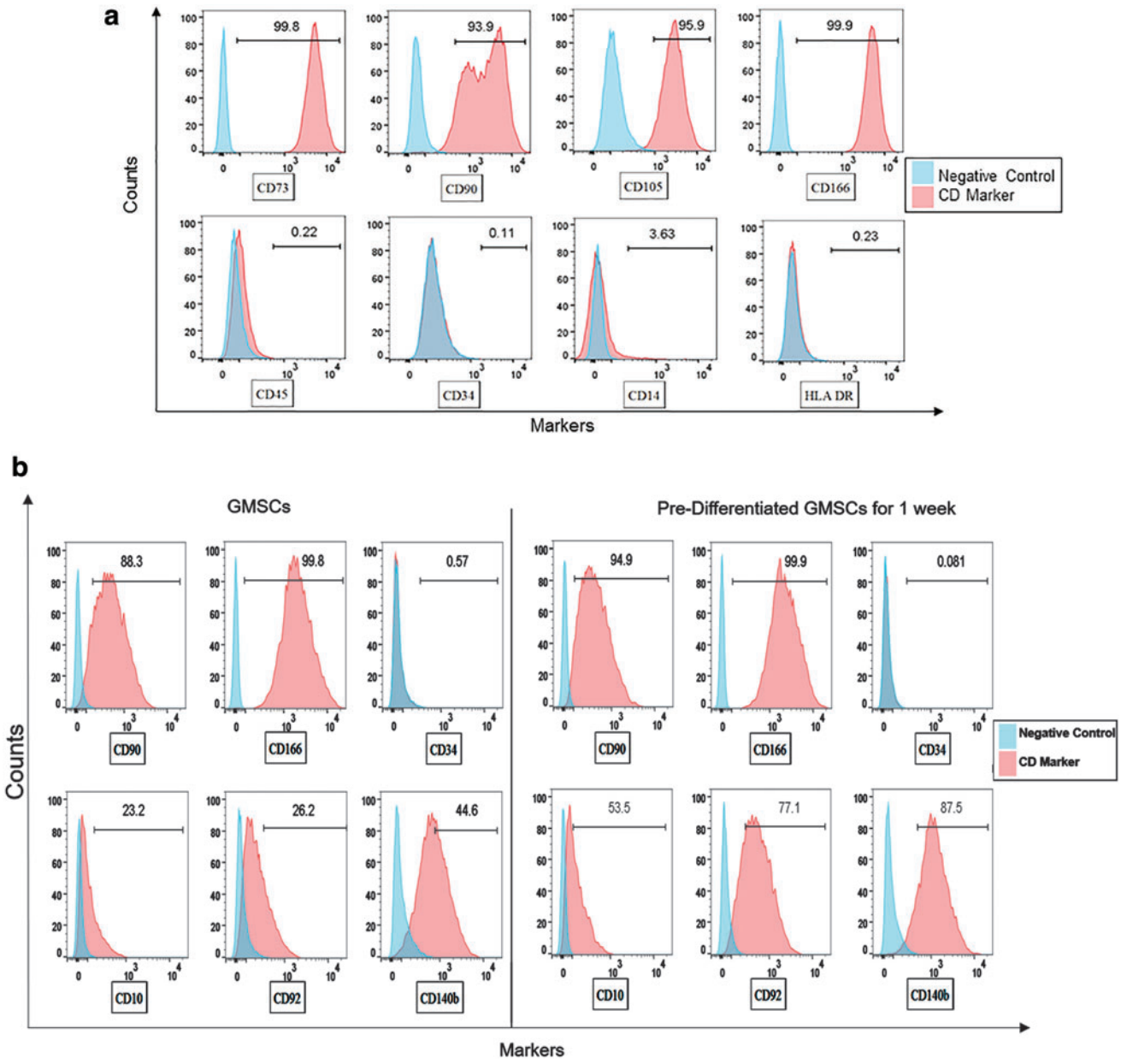

FIG. 1. **(a)** GMSCs were stained positive (>90%) for MSC surface markers CD73, CD105, CD90, CD166, and negative for hematopoietic markers CD45, CD34, CD14, and HLA DR. The expression of markers were in agreement with the criteria identified by the committee of International Society for Cellular Therapy. **(b)** GMSCs upon induction in osteogenic medium for a week showed increased expression of CD10 (Neprilysin), CD92 (choline transporter-like protein 1), and CD 140b (platelet-derived growth factor receptor beta) as compared with the undifferentiated GMSCs confirming the induction of osteogenic differentiation. The expression of CD90, CD166, and CD34 remained stable during differentiation. GMSC, gingiva-derived mesenchymal stem cell; MSC, mesenchymal stem cell. Color images are available online.

of appetite, and weight loss). For an analgesic purpose, buprenorphine (0.1–0.05 mg/kg) was administered subcutaneously at 12-h intervals for the first 72 h. The animals were provided with a soft diet for the first 3 days. Animals were euthanized at 4 and 8 weeks for postmortem analyses.

GMSCs culture and characterization

The collection of gingival tissue was performed in accordance with the Declaration of Helsinki and approved by the Institutional Review Board Committee (#02071304) at NSU. The excess gingival tissue during the crown lengthening or tooth extraction procedure, otherwise discarded, was collected from the dental clinic of the College of Dental Medicine at NSU.

MSCs were isolated from the gingival tissue using previously established procedures.[14] The isolated GMSCs were cultured in growth media (Dulbecco's Modified Eagle Medium containing 10% fetal bovine serum [FBS] and 1% antibiotics) at 37°C in 5% CO_2. The first two passages were allowed to further expand, and the cells in the third or fourth passages were used for experiments. To induce osteogenic differentiation, the cells at 70–80% confluence were stimulated with

osteogenic supplements, including 50 μg/mL ascorbic acid, 10 mM β glycero phosphate, and 100 nM dexamethasone in growth medium for a week.

These predifferntiated GMSCs and undifferentiated GMSCs were then analyzed for their expression of mesenchymal and lineage-specific surface markers by a flow cytometer.

GMSCs grown in the tissue culture flask were detached by trypsinization and washed twice with cold fluorescence-activated cell sorting buffer containing 5% FBS. Single cell suspensions were incubated for 20 min in the dark at +4°C with specific anti-human antibody conjugated with fluorochrome according to manufacturer's instructions as listed in Table 1. Before incubation with the antibodies, the cells were incubated with Human FcR Blocking Reagent (BD Biosciences, San Jose, CA) for 10 min. Unstained cells were used as negative control to set the voltages and negative gates appropriately. At least 15,000 events were acquired for each sample using BD LSR Fortessa X-20 cell analyzer, followed by postanalysis using FlowJo software.

Formulation of injectable dGMSCs-scaffold mixture

A commercially available self-assembling nanofiber hydrogel scaffold, PM (Corning, NY), was employed for this study. Our pilot data indicated that the GMSCs encapsulated in 0.5% PM demonstrated the most efficient proliferation and attachment within the gel. The GMSCs were predifferentiated to osteogenic precursors *in vitro* by induction with osteogenic supplements for 7 days.[6,21] The dGMSCs were suspended at 1×10^6 in 15 μL of serum-free medium and then mixed with 15 μL of 1% PM gel.[21,22] Using a pipette tip, the dGMSCs-PM mixture, with or without 2 μg/mL BMP2 (R&D Systems, Minneapolis, MN) was slowly drawn into the bone defect created in rats. The control defect group received an injection of phosphate-buffered saline (PBS) into the bone defect. In all rat groups, the periosteal flaps were closed after the injection of GMSCs, either PM mixture or PBS.

We have assigned two different treatments to right and left side of alveolar bone surfaces, following the protocol established by other groups,[23,24] as follows: (1) rat group A: defect alone (left) and no defect (right), (2) rat group B: defect administered with PM/BMP2 + dGMSCs (left) and defect administered with PM alone (right), (3) rat group C: defect administered with PM/BMP2/dGMSCs (left) and defect administered with PM/dGMSCs (right), (4) rat group D: defect administered with PM/BMP2/dGMSCs (left) and defect administered with PM/BMP2 (right).

Microcomputed tomography analysis

Quantitative bone morphometry analyses were performed on the euthanized rats using a high-resolution microcomputed tomography (micro-CT, SkyScan 1176; Bruker, Billerica, MA). The animals were scanned at 80 kV and 313 mA through 360°C with resolution of 17 μm and 0.5 rotation step, using a 0.5 mm aluminum filter. Bone healing was monitored at 4 and 8 weeks postsurgery using micro-CT. The cross-sectional views of digitally captured images were processed by the NRecon program (Bruker). Three-dimensional images were analyzed by Bruker's CTAN software. The measured bone volume was expressed in mm^3.

Histology and immunohistochemistry

The maxillary jaw involving the bone defect site was dissected from euthanized rats at 4 and 8 weeks. After fixation in 10% buffered formalin, the collected samples were decalcified and sectioned in paraffin blocks for Hematoxylin and Eosin (H&E) staining and Masson's Trichrome staining (FirstPath Laboratory Services, Pompano Beach, FL).

For immunohistochemistry, the sections (5 μm thick) were deparaffinized and endogenous peroxidase activity was inhibited with 3% hydrogen peroxide. The primary antibodies, human anti-osteocalcin (OCN) antibody (1:200 dilution; Thermo Fisher, Waltham, MA) to detect OCN and an antibody against human mitochondria (1:100 dilution; Fisher Scientific, Waltham, MA) were used to identify the human origin of implanted graft. Immunostaining was

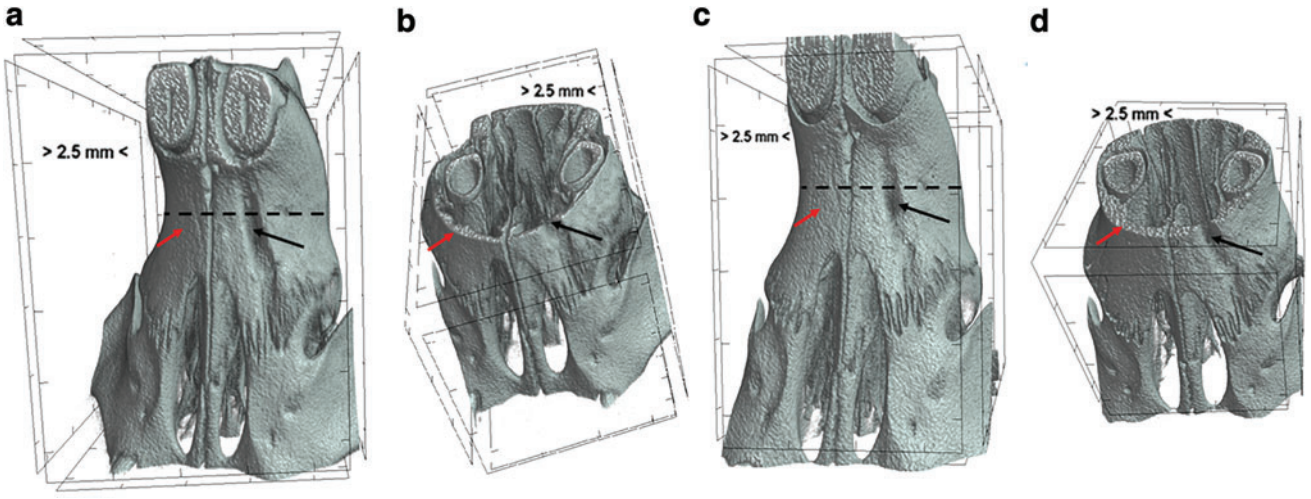

FIG. 2. Microcomputed images (micro-CT) data showing defect group. **(a)** 4 weeks postsurgery; **(b)** axial section of the rat head showing defect at week 4 **(c)** 8 weeks after surgery; **(d)** axial section showing rat head showing defect at one side and no defect (no surgical intervention) at other side. There was no spontaneous bone regeneration in the defect area at either 4 or 8 weeks. The *red arrow* represents no defect (no surgical intervention) area and *black arrow* represents surgically made defect. *Broken black line* indicates the axial section that was represented in **(b, d)**. micro-CT, microcomputed tomography. Color images are available online.

detected by the Universal Immunoperoxidase (horseradish peroxidase) ABC Kit (Vector Laboratories, Burlingame, CA). The diaminobenzidine substrate (Millipore Sigma, St. Louis, MA) was used as chromogen, followed by Hematoxylin counter stain. Digital images were obtained for histology and immunohistochemistry using a Leica microscope (Buffalo Grove, IL) equipped with a charge-coupled device camera (Olympus, Center Valley, PA).

Statistical analysis

The data were expressed in mean ± standard deviation. Statistical analysis was performed through a one-way analysis variance using GraphPad Prism (GraphPad Software, Inc., La Jolla, CA). Tukey's multiple comparison was performed for intergroup comparisons. The criterion for statistical significance was $p < 0.05$.

Results

Phenotypic characterization of GMSCs

Flow cytometric analysis demonstrated that expressions of typical MSC surface markers, CD73, CD105, CD90, and CD166 were expressed at high incidence (>90%) in the undifferentiated GMSCs, whereas the hematopoietic markers CD45, CD34, CD14, and HLA-DR were expressed <0.4% of the GMSCs (Fig. 1a), suggesting that the GMSCs established in this study are highly enriched with MSC, with little or no existence of hematopoietic stem cells.

Next, undifferentiated GMSCs and predifferentiated GMSCs were compared for their expressions of CD10 (Neprilysin), CD92 (choline transporter-like protein 1), and CD140b/platelet-derived growth factor receptor beta (PDGFR-β), all of which are known to be upregulated during osteogenic differentiation.[25] Markedly increased

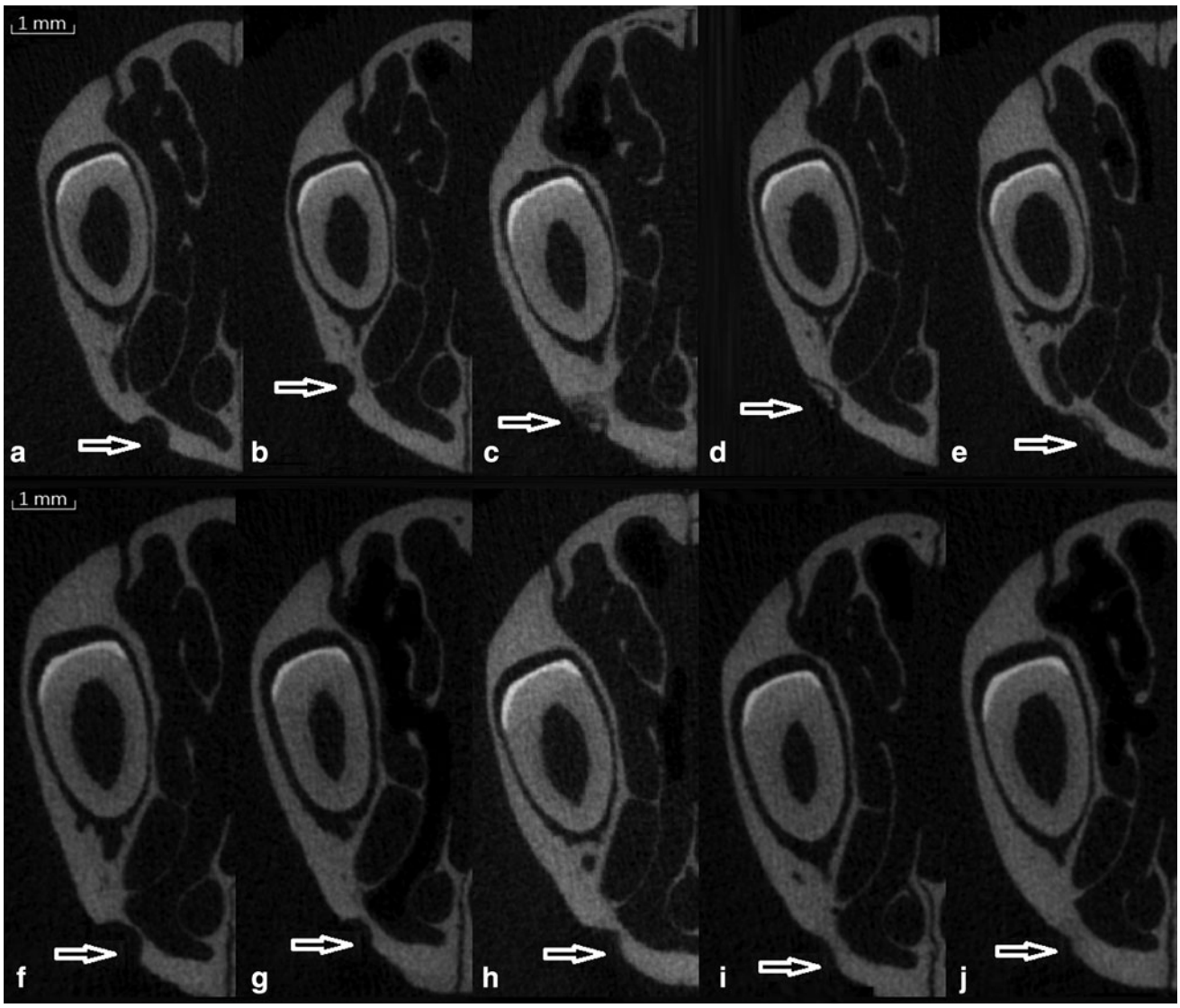

FIG. 3. micro-CT pictures showing the bone regeneration ability of various groups. **(a–e)** Four weeks postsurgery, **(f–j)** 8 weeks postsurgery; *arrows* represent the defect area, **(a)** defect, **(b)** PM, **(c)** PM/BMP2, **(d)** PM/GMSCs, **(e)** PM/dGMSCs/BMP2, **(f)** defect, **(g)** PM, **(h)** PM/BMP2, **(i)** PM/dGMSCs, and **(j)** PM/dGMSCS/BMP2. There was no spontaneous healing in the defect group **(a)** either at 4 or 8 weeks. All other groups showed bone healing. PM/dGMSCs/BMP2 group **(j)** filled the bone volume completely at 8 weeks. PM, Puramatrix™; BMP2, bone morphogenetic protein 2; dGMSC, predifferentiated GMSC.

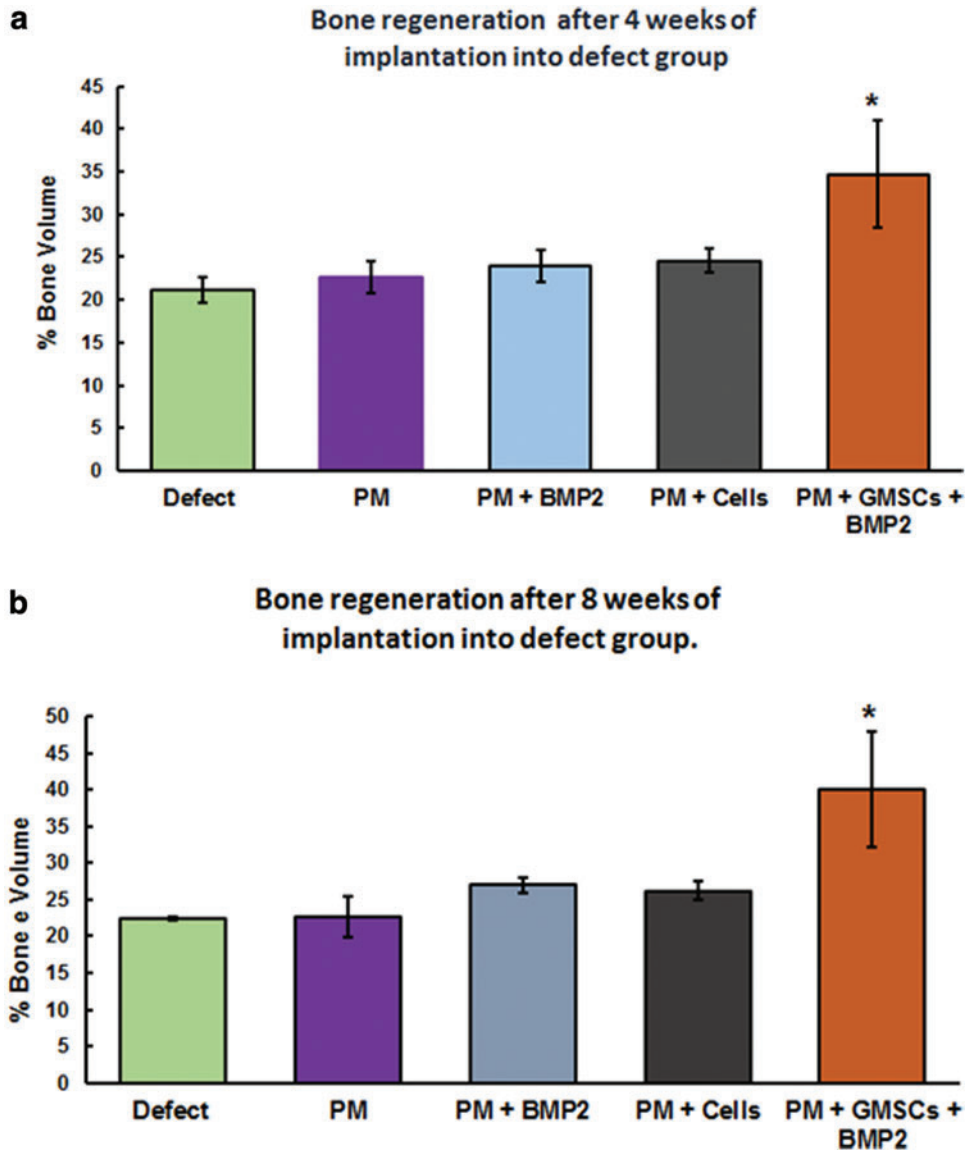

FIG. 4. Quantitative analysis of micro-CT data showing % bone volume at week 4 and 8 postsurgery. *X*-axis represents the groups and *Y*-axis indicates the % bone volume. The results were expressed as % bone volume. Control defect group was compared with experimental groups. The bone regenerated in all experimental groups, however, there was no significant difference between control and PM group, PM + dGMSCs, or PM + BMP2 either at 4 or 8 weeks. There was significant increase in the bone volume in PM + dGMSCs + BMP2 group at 4 and 8 weeks compared with control and all other groups ($p < 0.0001$). **(a)** 4 weeks, **(b)** 8 weeks. Error bars represent standard deviation. *Depicts statistical difference between control defect group and PM/BMP2/dGMSCs. Color images are available online.

expressions of CD10 (30.3% increase), CD92 (50.8% increase), and CD140b (42.9% increase) were seen in dGMSCs compared with undifferentiated GMSCs (Fig. 1b). It is noteworthy that the expression patterns of MSC markers (CD90 and CD166) and hematopoietic stem cell marker (CD34) were comparable between undifferentiated GMSCs and dGMSCs (Fig. 1b).

micro-CT analysis

The digitally captured images of maxillary bone using a micro-CT were reconstructed to two-dimensional and three-dimensional images and the bone morphometric parameters were quantitated using the CTAN program. The results were expressed as percent bone volume = (originally created defect volume − defect volume at 4-week or 8-week]/original bone defect volume) × 100. In control defect group, no spontaneous bone regeneration was observed either at 4 or at 8 weeks (Figs. 2a–d, and 3a, f). No significant increase in percent bone volume was detected between 4 and 8 weeks in any of the groups.

Data of PM/dGMSCs and PM/BMP2 groups demonstrated no significant difference in bone volume filling between these two groups (Fig. 4a, b). Newly regenerated bone in the composition of PM/dGMSCs/BMP2, however, showed significant increase (34.6 ± 6.2) over that of the control defect group (21.2 ± 1.4) at 4 weeks. At 8 weeks, the PM/dGMSCs/BMP2 group showed significant enhancement (40.1 ± 7.1) compared with the defect group (22.4 ± 0.16). Overall, results showed the maximum increase in bone volume in the PM/dGMSCs/BMP2 group at 4 and 8 weeks compared with all other groups (Fig. 4a, b). Bone volume filling the defect slightly progressed with no statistical significance from 4 to 8 weeks, and at 8 weeks, complete bone volume filling was observed in the PM/dGMSCs/BMP2 group (Fig. 3e, j).

Histology and immunohistochemistry

The bone formation was evaluated by H&E staining and the development of new bone within the defect was determined by the presence of lamellar bone formation and the presence of vascularization, as well as live osteocytes and osteoblasts.

The alveolar defects that were left empty in the control defect group did not heal spontaneously either at 4 or 8 weeks indicating that the surgical defect created in this rat model was a critical size defect (Fig. 5a–d). Loose connective tissue was noted in the control defect site accompanied by fibroblasts and small blood vessels at 8 weeks (Fig. 5b, d). Compared with the control defect group, all the treatment groups showed new bone formation with the presence of osteoblast-like cells on the surface of newly formed bone (Fig. 5a–t).

PM supported the new bone formation to a certain extent at 4 and 8 weeks (Fig. 5e–h). The PM/BMP2 showed the lamellar bone formation after 4 weeks followed by matured bone after 8 weeks (Fig. 5i–l). The PM/dGMSCs group at 4 weeks showed live osteocytes within lacunae, osteoblasts lining the peripheral portion of the newly formed bone, and immature blood vessels developing within the new bone (Fig. 5m, n) followed by more matured bone at 8 weeks (Fig. 5o, p), with lining of osteoblasts throughout the newly formed bone (Fig. 5q–t).

Newly formed bone in the PM/dGMSCs/BMP2 group exhibited a lamellar organization with osteocytes and new vascularization in the defect at 4 weeks (Fig. 5q, r). Full integration was observed in newly formed bone with host bone tissue. The PM/dGMSCs/BMP2 group at 8 weeks showed more matured bone with reversal lines and neovascularization with the presence of osteocytes. Tight integration of new bone and host bone tissue was noted at 8 weeks (Fig. 5s, t). Masson's Trichrome staining showed new bone formation at 4 weeks and followed by more matured bone at 8 weeks in the PM/BMSCs/dGMSCs group (Fig. 6a, b).

Immunohistochemical staining demonstrated a strong expression of OCN in newly formed bone. The positive immunostaining in mitochondria in the cells confirmed the human origin. The acellular bone on the other hand showed negative staining to human mitochondria (Fig. 7a, b).

Discussion

The advent of stem cell-based bone regeneration is offering many solutions for the repair of complicated defects in the craniofacial region. Nonetheless, currently available stem cell-based approaches are only feasible in regenerating small-sized bone defects. This calls for the suitable stem cells and scaffolding material to regenerate the bone in critical size defects. This study utilized the surgically created critical defect in nude rat model to test the osteogenic potential of dGMSCs loaded in a nanofiber hydrogel.

An animal model to simulate the critical size bone defect found in the craniofacial region of human patients is essential. A number of *in vivo* models using animals, such as rats,[4,10,26] rabbits,[27] dogs,[8] juvenile swine,[7] and nonhuman primates,[28] have been developed to test the potency of the stem cell-based regenerative approach for alveolar cleft. Despite some practical difficulties involved, small rodent models have added advantages, such as, cost effectiveness and easy handling.[5] In the present study, a critical size (7 mm × 1 mm × 1 mm) defect was created in the alveolar bone of nude rats with slight modifications to the published protocol,[26] and the bone regenerative potential of dGMSCs was evaluated.

The size of the alveolar bone defect in various rat models varied. While Mehrara *et al.*[29] reported that a 9 mm × 5 mm × 3 mm defect created in alveolar bone of rats (strain unknown) as an alveolar cleft model, Nguyen *et al.*[30] reported a defect size of 7 mm × 4 mm × 3 mm created in Wistar and Sprague Dawley rats as the critical size alveolar cleft. However, both former and latter models[29,30] caused substantial injury to the surrounding tissues, which resulted in the failure to test bone graft techniques.[26,31] For these reasons, Mostafa *et al.* discovered that smaller sizes, that is, 5 mm × 2.5 mm × 1 mm, created in alveolar bone of Wistar

FIG. 5. Histological assessment of bone regeneration at 4 and 8 weeks postimplantation. Sections stained with Hematoxylin and Eosin. For all pictures *left panel* showing low magnification (5×) *right panel* showing higher magnification (20×) with scale bar 100 μm and magnified view is 20 μm**. (a–d)** Control defect group**:** Figure showing surgical defect made in the alveolus region **(a)** 4 weeks postsurgery, the entire defect area is shown. **(b)** Magnified view of control defect site. Very thin lining of osteoblasts at the defect area is seen. **(c)** Eight-weeks postsurgery; the entire defect site was shown. The *arrow* indicates the presence of connective tissue. **(d)** Magnified view of defect area, the control defect site showed only thin band of fibrous connect tissue around and there was no spontaneous healing observed, which confirms that the critical size defect**. (e–h)** PM group **(e)** 4 weeks postsurgery, showing the hydrogel material attached to newly formed bone, surrounded by connective tissue, small portion of lamellar bone is seen, **(f)** magnified view showing lamellar bone formation with osteocytes. The newly formed bone is covered by hydrogel, **(g)** 8 weeks postsurgery showed a lamellar bone with the presence of osteoblasts, **(h)** (magnified view) remnants of hydrogel is seen. **(i–l)** PM/BMP2 group **(i)** 4 weeks postsurgery, showing the lamellar bone formation with remnants of hydrogel material, **(j)** magnified view showing newly formed bone. Although, PM/BMP2 could not fill the bone volume, PM in the presence of BMP2 enhanced bone formation **(k)** 8 weeks postsurgery showed a lamellar bone with the presence of osteoblasts, **(l)** magnified view showing osteoblasts. **(m–p)** PM/dGMSCs group **(m)** 4 weeks postsurgery, showing lamellar bone with connective tissue around. **(n)** Magnified view 4 weeks postsurgery showed more matured bone with live osteocytes within lacunae, osteoblasts lining the peripheral portion of the newly formed bone, and immature blood vessels developing within the new bone. **(o)** 8 weeks post surgery showing more matured bone, with connective tissue attached **(p)** the enlarged view showing osteoblast lining and osteocytes. **(q–t)** PM/GMSCs/BMP2 group **(q)** 4 weeks after the surgery; more bone fill is seen in this group than the other group. **(r)** The integration of newly formed host bone is seen **(s)** 8 weeks after surgery **(t)** more matured bone is seen with reversal lines. Color images are available online.

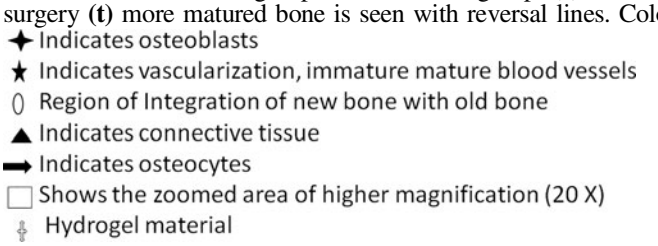

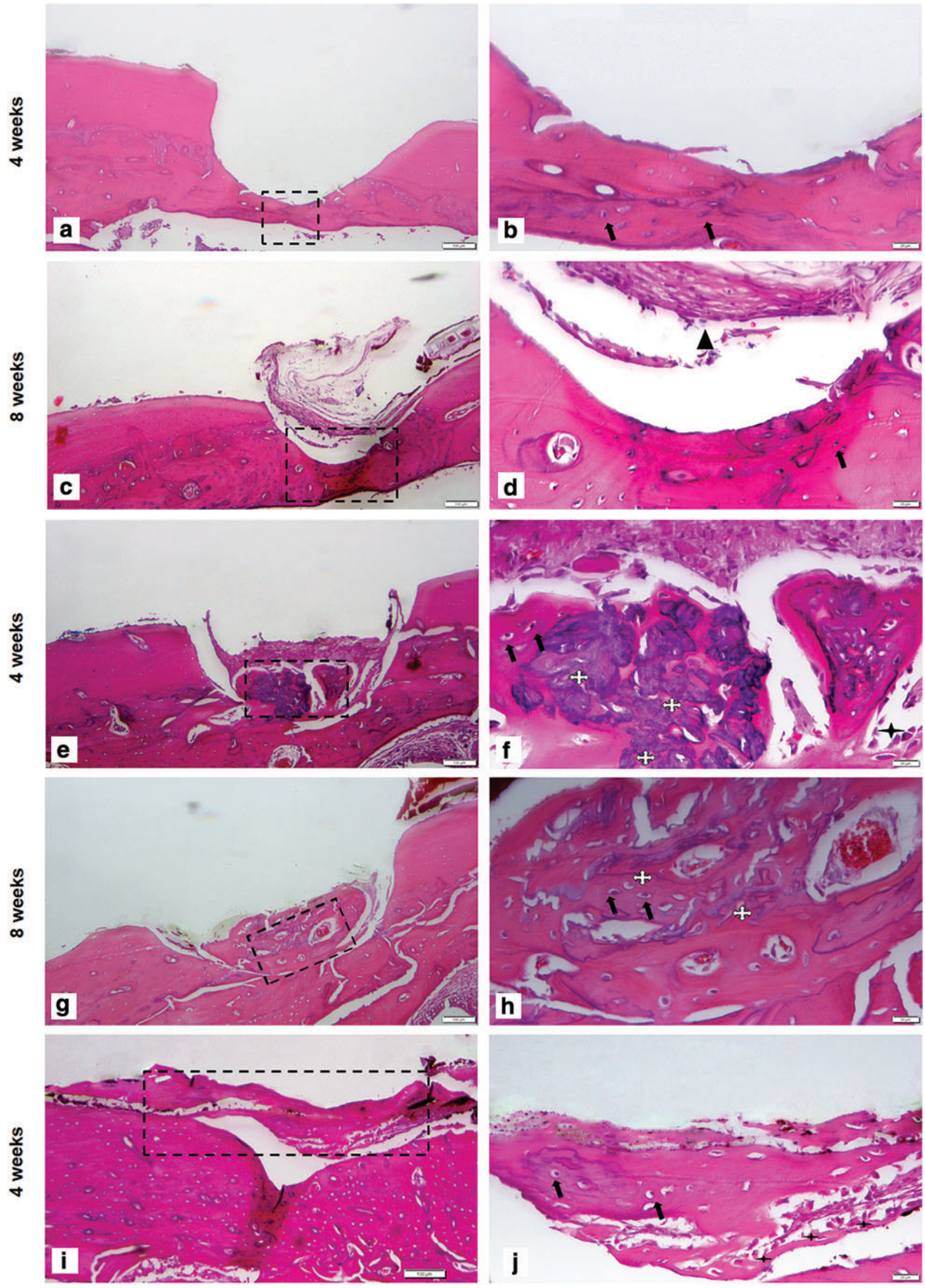

FIG. 5. (Continued).

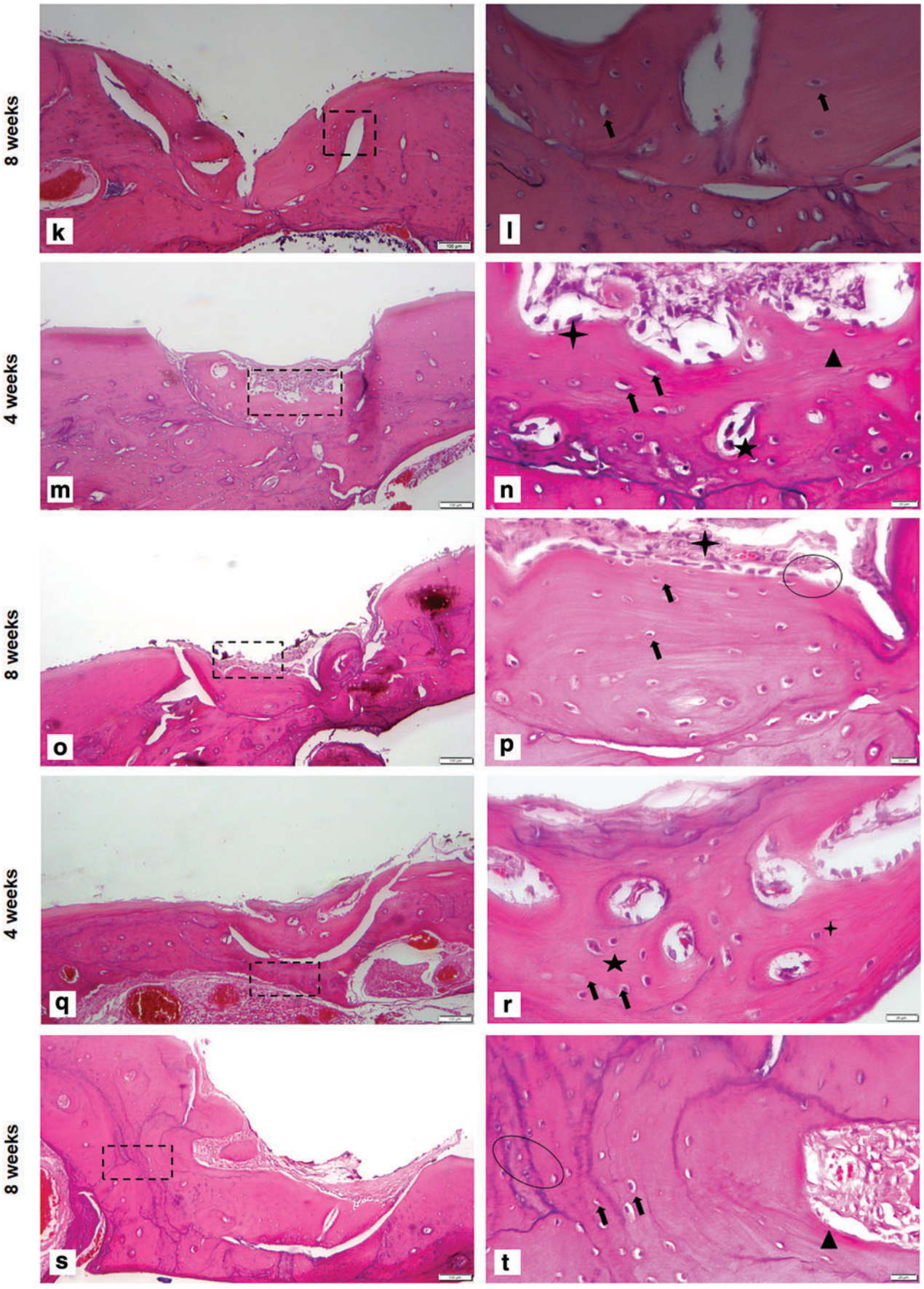

FIG. 5. (Continued).

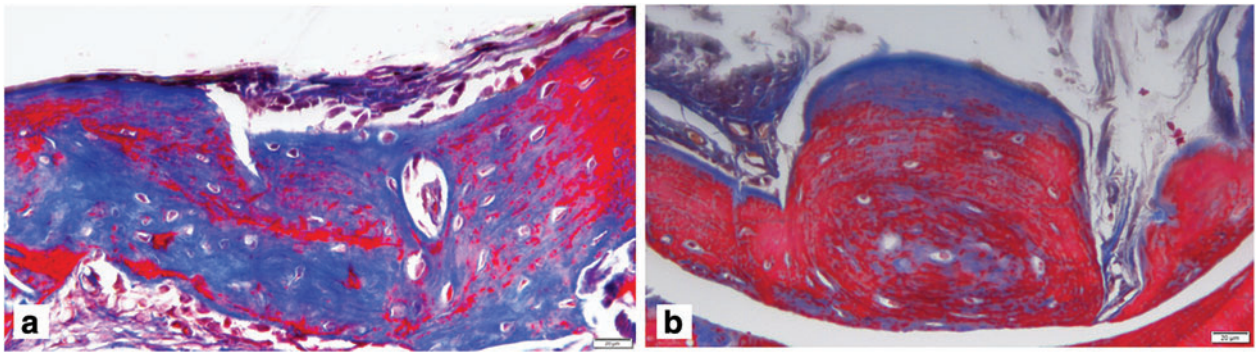

FIG. 6. Masson's Trichrome staining PM/GMSCs/BMP2 group **(a)** 4 weeks large amount of new bone formation is seen (*blue* area indicates new bone formation **(b)** 8 weeks postsurgery of implantation, more mature bone is seen. Color images are available online.

and Sprague Dawley rats would minimize the collateral damages to adjacent tissue.[26]

Based on our pilot studies, we chose to create much smaller critical size defect in the alveolar region of nude rats, specifically, 7 mm × 1 mm × 1 mm, compared with critical size determinations in the above three studies.[26,29,30] This size in alveolar bone allowed the controlled application and retention of graft material, and it prevented the collateral injury to the nasal floor. Very importantly, the nude rats with defect alone showed no bone growth at the 4 and 8 weeks, as determined by micro-CT analysis (Fig. 3a, f) and histological evaluation (Fig. 5a–d), suggesting that 7 mm × 1 mm × 1 mm was indeed, the smallest critical size defect that could be created in the alveolar bone of rats. Collectively, the critical size defect that we created is the smallest size tested in a rat maxillary alveolar region.

The micro-CT data revealed that the PM alone group could not induce defect healing over 8 weeks. However, PM supported the bone formation in combination with both BMP2 and/or GMSCs (Fig. 3c, d, h, and i). Importantly, the PM/GMSCs/BMP2 group showed significant enhancement of new bone formation compared with other formulations tested.

Histological results were consistent with the results from micro-CT analysis. In the absence of a cell-scaffold system, histological analysis revealed that the control defect group failed to heal, even after 8 weeks, and a fibrous layer covered a part of the defect (Fig. 5a–d). This is expected in critical size defects as a large amount of bone is removed, and the periosteum is no longer intact. Additionally, owing to the lack of supporting tissue around the defect, the cellular infiltration and tissue formation might not occur.[32,33]

In agreement with the micro-CT data, histological results showed enhanced bone formation in the PM/dGMSCs/BMP2 group (Fig. 5q–t). In our study, bone formation was seen in all experimental groups, including PM, PM/dGMSCs, PM/BMP2, and PM/dGMSCs/BMP2 groups at 4 weeks postimplantation. These results were consistent with published data on deciduous dental pulp stem cells.[10]

Our immunohistochemical analysis revealed the presence of OCN (Fig. 7b). OCN, the most abundant protein in the bone, produced by osteoblasts.[34] Under mineralized condition osteoblasts increase OCN production upto 20-fold.[35] OCN, the newly regenerated bone showed positive to OCN antibody. The human origin was confirmed by the presence of human mitochondria in newly formed bone.

The GMSCs used in this study exhibited the uniform fibroblast-like morphology, expressed high levels of MSC-distinct surface antigens, such as CD73, CD105, CD90, and CD166, and did not express hematopoietic lineage markers CD14, CD34, CD45, and HLA-DR, thus confirming the MSCs phenotype as previously described.[36] In this study, we adopted a protocol of short-term osteoinduction (7 days) before the transplantation of the GMSCs in the alveolar

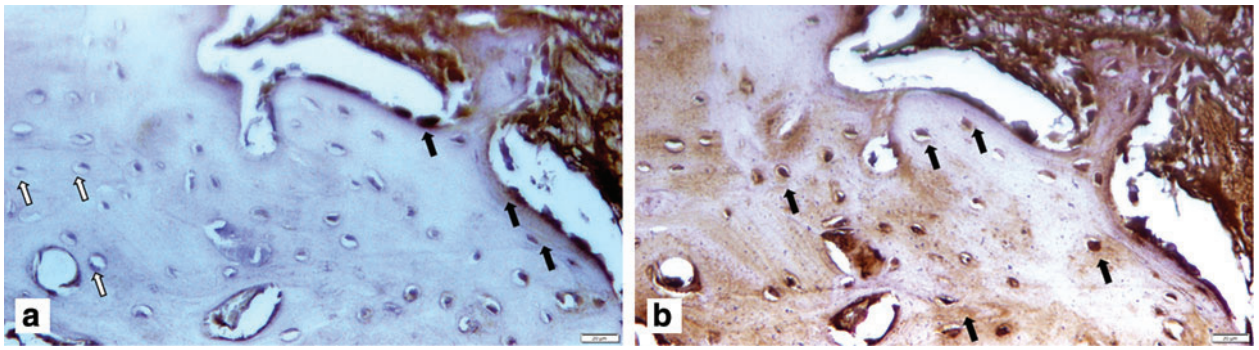

FIG. 7. The survival and osteogenesis of grafted dGMSCs in the defect area after 4 weeks of the surgery was detected by immunohistochemical staining with anti-osteocalcin antibody. GMSCs human origin was detected with a specific antibody for human mitochondria (*black arrows*). **(a)** Defect area after 4 weeks of surgery without GMSC implantation served as negative control. The absence of expression to anti-human mitochondria and osteocalcin can be seen. Color images are available online.

defect site to provide necessary osteoinductive cues.[22,37–39] Moreover, locally applied osteogenic progenitor cells enhance osteogenesis compared with untreated MSCs.[6,40] In our study, GMSCs exposed to osteogenic medium for a week, resulted in increased expression of CD10, CD92, and CD140b compared with the untreated GMSCs, consistent with the published report[25]; while maintaining the MSC phenotypic markers (CD90 and CD166). CD10, a cell surface metallo-endopeptidase enzyme, is expressed by osteoblasts in both *in vivo* and *in vitro* contexts to participate in osteogenesis by catalytic generations of such osteogenic growth peptides as calcitonin and osteostatin.[41] The main function of CD92 is to transport choline, which is then incorporated into phosphatidyl choline (PC) across the cell membrane. PC is known to increase the osteoconductivity of the bone by osteoblasts.[42] CD140b, also known as PDGFR-β, is involved in the regulation of bone formation. In sum, the phenotypic expression of dGMSCs confirms their induction toward osteogenic lineage (Fig. 1b).

The success of bone tissue engineering relies on osteogenic cells, osteoconductive scaffolds, and osteoinductive signals. Bone morphogenetic protein (BMP2), an osteogenic inducer, is known to enhance the bone healing of MSCs in many bone defect models.[43–46] Stem cells derived from dental tissues implanted in a bone defect in the absence of growth factor showed incomplete filling of new bone at 8 weeks postsurgery.[10,47] Thus, we hypothesized that BMP2 might support the bone formation ability of GMSCs. Our data showed that the use of BMP2 facilitated further acceleration of bone regeneration in GMSCs and assisted in complete bone volume filling at 8 weeks postsurgery (Fig. 2j) in the defect site. Conventionally, while BMP2 is used in supraphysiological doses in many clinical applications,[48,49] it has shown adverse effects, such as enhanced bone formation in undesired sites, inflammation, and respiratory distress.[48–51] In this study, we used lower doses of BMP2 (2 μg/mL) as compared with other studies (11, 1, and 8 μg/mL).[52,53]

In summary, we have established a proof of concept of regenerative ability of GMSCs in critical size craniofacial defects. The model developed in this study provides a reproducible critical size defect and allows evaluating the mechanism of accelerated wound healing and regeneration of bone using tissue-engineering strategies. Furthermore, the hydrogel used in combination with GMSCs and BMP2 supported bone healing and provided the architecture to maintain the cells at the surgical site. However, GMSCs used in this study were from a single donor, and an autogenous bone graft was not used to compare the efficacy of GMSCs. While many studies have reported the methods of generating clinical grade MSCs from various tissues such as bone marrow, umbilical cord etc. with good manufacturing practices (GMP) for collection, preservation, and culture,[54,55] GMP grade GMSCs are yet to be established. Currently, manufacturing cells under xenofree and Current GMP conditions are a major barrier for further advancement of personalized regenerative medicine. Further efforts are needed for the translation of this technology to the clinics.

Conclusions

This study demonstrated that combination of predifferentiated osteogenic GMSCs (dGMSCs), self-assembling hydrogel and low doses of BMP2 accelerated bone regeneration in a rat model of alveolar bone defect, suggesting that dGMSCs may lead to novel cell therapy for enhanced bone regeneration in alveolar cleft and other bone defect complications in craniofacial area. Furthermore, the critical size defect that we created appears to be the smallest size tested in a rat maxillary alveolar region, representing several advantages, including (1) the avoid of injury to the surrounding tissues, (2) the secured space to retain the transplanted cells, and (3) increased reproducibility. Thus, our study has potential for future advances in *in-situ* gelling matrix models and facilitate regeneration of alveolar bone defects, which are affordable and patient compliant.

Acknowledgments

The authors thank Mohamed Kaplan (animal surgery), Mr. Josh Samuel (microCT scanning), Mr. Jerry Ennolikara (histology), Dr. Lynn W. Solomon (histology), and Alaa K. Redwan (figures) for their assistance.

Disclosure Statement

No competing financial interests exist.

Funding Information

This study was supported by Oral and Maxillofacial Foundation Grant, Presidents' Faculty Research & Development Grant at Nova Southeastern University, and National Institute of Dental Health and Craniofacial Research R15 grant (DE027851).

References

1. Meng, L. Biological mechanisms in palatogenesis and cleft palate. J Dent Res **88,** 22, 2009.
2. Shahnaseri, S., Sheikhi, M., Hashemibeni, B., Mousavi, S.A., and Soltani, P. Comparison of autogenous bone graft and tissue-engineered bone graft in alveolar cleft defects in canine animal models using digital radiography. Indian J Dent Res **31,** 118, 2020.
3. Wang, X., Xing, H., Zhang, G., *et al.* Restoration of a critical mandibular bone defect using human alveolar bone-derived stem cells and porous nano-HA/collagen/PLA scaffold. Stem Cells Int **2016,** 8741641, 2016.
4. Korn, P., Schulz, M.C., Range, U., Lauer, G., and Pradel, W. Efficacy of tissue engineered bone grafts containing mesenchymal stromal cells for cleft alveolar osteoplasty in a rat model. J Craniomaxillofac Surg **42,** 1277, 2014.
5. Kim, J.H., Moon, H.J., Kim, T.H., *et al.* A novel in vivo platform for studying alveolar bone regeneration in rat. J Tissue Eng **4,** 2041731413517705, 2013.
6. Caballero, M., Jones, D.C., Shan, Z., Soleimani, S., and van Aalst, J.A. Tissue engineering strategies to improve osteogenesis in the juvenile swine alveolar cleft model. Tissue Eng Part C Methods **23,** 889, 2017.
7. Caballero, M., Morse, J.C., Halevi, A.E., *et al.* Juvenile swine surgical alveolar cleft model to test novel autologous stem cell therapies. Tissue Eng Part C Methods **21,** 898, 2015.
8. Yuanzheng, C., Yan, G., Ting, L., Yanjie, F., Peng, W., and Nan, B. Enhancement of the repair of dog alveolar cleft by an autologous iliac bone, bone marrow-derived mesen-

chymal stem cell, and platelet-rich fibrin mixture. Plast Reconstr Surg **135,** 1405, 2015.
9. Lin, C.Y., Kuo, P.J., Chin, Y.T., *et al.* Dental pulp stem cell transplantation with 2,3,5,4′-tetrahydroxystilbene-2-*O*-beta-D-glucoside accelerates alveolar bone regeneration in rats. J Endod **45,** 435, 2019.
10. Jahanbin, A., Rashed, R., Alamdari, D.H., *et al.* Success of maxillary alveolar defect repair in rats using osteoblast-differentiated human deciduous dental pulp stem cells. J Oral Maxillofac Surg **74,** 829.e1, 2016.
11. Fournier, B.P., Loison-Robert, L.S., Ferre, F.C., Owen, G.R., Larjava, H., and Hakkinen, L. Characterisation of human gingival neural crest-derived stem cells in monolayer and neurosphere cultures. Eur Cell Mater **31,** 40, 2016.
12. Al-Qadhi, G., Soliman, M., Abou-Shady, I., and Rashed, L. Gingival mesenchymal stem cells as an alternative source to bone marrow mesenchymal stem cells in regeneration of bone defects: in vivo study. Tissue Cell **63,** 101325, 2020.
13. Sun, Q., Nakata, H., Yamamoto, M., Kasugai, S., and Kuroda, S. Comparison of gingiva-derived and bone marrow mesenchymal stem cells for osteogenesis. J Cell Mol Med **23,** 7592, 2019.
14. Tomar, G.B., Srivastava, R.K., Gupta, N., *et al.* Human gingiva-derived mesenchymal stem cells are superior to bone marrow-derived mesenchymal stem cells for cell therapy in regenerative medicine. Biochem Biophys Res Commun **393,** 377, 2010.
15. Xu, X., Chen, C., Akiyama, K., *et al.* Gingivae contain neural-crest- and mesoderm-derived mesenchymal stem cells. J Dent Res **92,** 825, 2013.
16. Zhang, Q. Mesenchymal stem cells derived from human gingiva are capable of immunomodulatory functions and ameliorate inflammation-related tissue destruction in experimental colitis. J Immunol **183,** 7787, 2009.
17. Venkatesh, D., Kumar, K.P.M., and Alur, J.B. Gingival mesenchymal stem cells. J Oral Maxillofac Pathol **21,** 296, 2017.
18. Wang, F., Yu, M., Yan, X., *et al.* Gingiva-derived mesenchymal stem cell-mediated therapeutic approach for bone tissue regeneration. Stem Cells Dev **20,** 2093, 2011.
19. Snider, T.N., and Mishina, Y. Cranial neural crest cell contribution to craniofacial formation, pathology, and future directions in tissue engineering. Birth Defects Res C Embryo Today **102,** 324, 2014.
20. Lin, H., Tang, Y., Lozito, T.P., Oyster, N., Wang, B., and Tuan, R.S. Efficient in vivo bone formation by BMP-2 engineered human mesenchymal stem cells encapsulated in a projection stereolithographically fabricated hydrogel scaffold. Stem Cell Res Ther **10,** 254, 2019.
21. Zhang, W., Zhang, Z., Chen, S., Macri, L., Kohn, J., and Yelick, P.C. Mandibular jaw bone regeneration using human dental cell-seeded tyrosine-derived polycarbonate scaffolds. Tissue Eng Part A **22,** 985, 2016.
22. Petridis, X., Diamanti, E., Trigas, G., Kalyvas, D., and Kitraki, E. Bone regeneration in critical-size calvarial defects using human dental pulp cells in an extracellular matrix-based scaffold. J Craniomaxillofac Surg **43,** 483, 2015.
23. Chamieh, F., Collignon, A.M., Coyac, B.R., *et al.* Accelerated craniofacial bone regeneration through dense collagen gel scaffolds seeded with dental pulp stem cells. Sci Rep **6,** 38814, 2016.
24. Suenaga, H., Furukawa, K.S., Suzuki, Y., Takato, T., and Ushida, T. Bone regeneration in calvarial defects in a rat model by implantation of human bone marrow-derived mesenchymal stromal cell spheroids. J Mater Sci Mater Med **26,** 254, 2015.
25. Graneli, C., Thorfve, A., Ruetschi, U., *et al.* Novel markers of osteogenic and adipogenic differentiation of human bone marrow stromal cells identified using a quantitative proteomics approach. Stem Cell Res **12,** 153, 2014.
26. Mostafa, N.Z., Doschak, M.R., Major, P.W., and Talwar, R. Reliable critical sized defect rodent model for cleft palate research. J Craniomaxillofac Surg **42,** 1840, 2014.
27. Kamal, M., Andersson, L., Tolba, R., *et al.* A rabbit model for experimental alveolar cleft grafting. J Transl Med **15,** 50, 2017.
28. Wang, L., Xu, W., Chen, Y., and Wang, J. Alveolar bone repair of rhesus monkeys by using BMP-2 gene and mesenchymal stem cells loaded three-dimensional printed bioglass scaffold. Sci Rep **9,** 18175, 2019.
29. Mehrara, B.J., Saadeh, P.B., Steinbrech, D.S., *et al.* A rat model of gingivoperiosteoplasty. J Craniofac Surg **11,** 54, 2000.
30. Nguyen, P.D., Lin, C.D., Allori, A.C., Ricci, J.L., Saadeh, P.B., and Warren, S.M. Establishment of a critical-sized alveolar defect in the rat: a model for human gingivoperiosteoplasty. Plast Reconstr Surg **123,** 817, 2009.
31. Nguyen, P.D., Lin, C.D., Allori, A.C., *et al.* Scaffold-based rhBMP-2 therapy in a rat alveolar defect model: implications for human gingivoperiosteoplasty. Plast Reconstr Surg **124,** 1829, 2009.
32. Zhang, X., Xie, C., Lin, A.S., *et al.* Periosteal progenitor cell fate in segmental cortical bone graft transplantations: implications for functional tissue engineering. J Bone Miner Res **20,** 2124, 2005.
33. Frohbergh, M.E., Katsman, A., Mondrinos, M.J., *et al.* Osseointegrative properties of electrospun hydroxyapatite-containing nanofibrous chitosan scaffolds. Tissue Eng Part A **21,** 970, 2015.
34. Zoch, M.L., Clemens, T.L., and Riddle, R.C. New insights into the biology of osteocalcin. Bone **82,** 42, 2016.
35. Deluiz, D., Delcroix, G.J., D'Ippolito, G., *et al.* Human bone marrow-derived mesenchymal stromal cell-seeded bone biomaterial directs fast and superior mandibular bone augmentation in rats. Sci Rep **9,** 11806, 2019.
36. Dominici, M., Le Blanc, K., Mueller, I., *et al.* Minimal criteria for defining multipotent mesenchymal stromal cells. The International Society for Cellular Therapy position statement. Cytotherapy **8,** 315, 2006.
37. van den Dolder, J., Vehof, J.W., Spauwen, P.H., and Jansen, J.A. Bone formation by rat bone marrow cells cultured on titanium fiber mesh: effect of in vitro culture time. J Biomed Mater Res **62,** 350, 2002.
38. Sikavitsas, V.I., van den Dolder, J., Bancroft, G.N., Jansen, J.A., and Mikos, A.G. Influence of the in vitro culture period on the in vivo performance of cell/titanium bone tissue-engineered constructs using a rat cranial critical size defect model. J Biomed Mater Res A **67,** 944, 2003.
39. Castano-Izquierdo, H., Alvarez-Barreto, J., van den Dolder, J., Jansen, J.A., Mikos, A.G., and Sikavitsas, V.I. Preculture period of mesenchymal stem cells in osteogenic media influences their in vivo bone forming potential. J Biomed Mater Res A **82,** 129, 2007.
40. Peters, A., Toben, D., Lienau, J., *et al.* Locally applied osteogenic predifferentiated progenitor cells are more effective than undifferentiated mesenchymal stem cells in the treatment of delayed bone healing. Tissue Eng Part A **15,** 2947, 2009.

41. Jones, E.A., Kinsey, S.E., English, A., *et al.* Isolation and characterization of bone marrow multipotential mesenchymal progenitor cells. Arthritis Rheum **46,** 3349, 2002.
42. Michel, V., and Bakovic, M. The solute carrier 44A1 is a mitochondrial protein and mediates choline transport. FASEB J 23, 2749, 2009.
43. Stephan, S.J., Tholpady, S.S., Gross, B., *et al.* Injectable tissue-engineered bone repair of a rat calvarial defect. Laryngoscope **120,** 895, 2010.
44. He, X., Liu, Y., Yuan, X., and Lu, L. Enhanced healing of rat calvarial defects with MSCs loaded on BMP-2 releasing chitosan/alginate/hydroxyapatite scaffolds. PLoS One **9,** e104061, 2014.
45. Del Rosario, C., Rodriguez-Evora, M., Reyes, R., Delgado, A., and Evora, C. BMP-2, PDGF-BB, and bone marrow mesenchymal cells in a macroporous beta-TCP scaffold for critical-size bone defect repair in rats. Biomed Mater **10,** 045008, 2015.
46. Kang, S.W., La, W.G., Kang, J.M., Park, J.H., and Kim, B.S. Bone morphogenetic protein-2 enhances bone regeneration mediated by transplantation of osteogenically undifferentiated bone marrow-derived mesenchymal stem cells. Biotechnol Lett **30,** 1163, 2008.
47. Moshaverinia, A., Chen, C., Xu, X., *et al.* Bone regeneration potential of stem cells derived from periodontal ligament or gingival tissue sources encapsulated in RGD-modified alginate scaffold. Tissue Eng Part A **20,** 611, 2014.
48. Jager, M., Fischer, J., Dohrn, W., *et al.* Dexamethasone modulates BMP-2 effects on mesenchymal stem cells in vitro. J Orthop Res **26,** 1440, 2008.
49. Kang, Q., Song, W.X., Luo, Q., *et al.* A comprehensive analysis of the dual roles of BMPs in regulating adipogenic and osteogenic differentiation of mesenchymal progenitor cells. Stem Cells Dev **18,** 545, 2009.
50. Gori, F., Thomas, T., Hicok, K.C., Spelsberg, T.C., and Riggs, B.L. Differentiation of human marrow stromal precursor cells: bone morphogenetic protein-2 increases OSF2/CBFA1, enhances osteoblast commitment, and inhibits late adipocyte maturation. J Bone Miner Res **14,** 1522, 1999.
51. Jorgensen, N.R., Henriksen, Z., Sorensen, O.H., and Civitelli, R. Dexamethasone, BMP-2, and 1,25-dihydroxyvitamin D enhance a more differentiated osteoblast phenotype: validation of an in vitro model for human bone marrow-derived primary osteoblasts. Steroids **69,** 219, 2004.
52. Lee, S.S., Huang, B.J., Kaltz, S.R., *et al.* Bone regeneration with low dose BMP-2 amplified by biomimetic supramolecular nanofibers within collagen scaffolds. Biomaterials **34,** 452, 2013.
53. Ben-David, D., Srouji, S., Shapira-Schweitzer, K., *et al.* Low dose BMP-2 treatment for bone repair using a PEGylated fibrinogen hydrogel matrix. Biomaterials **34,** 2902, 2013.
54. Hanley, P.J., Mei, Z., da Graca Cabreira-Hansen, M., *et al.* Manufacturing mesenchymal stromal cells for phase I clinical trials. Cytotherapy **15,** 416, 2013.
55. Dias, R.B., Guimarães, J.A.M., Cury, M.B., *et al.* The manufacture of GMP-grade bone marrow stromal cells with validated *in vivo* bone-forming potential in an orthopedic clinical center in Brazil. Stem Cells Int **2019,** 2608482, 2019.

Address correspondence to:
Umadevi Kandalam, PhD
Department of Oral Sciences and Translational Research
College of Dental Medicine
Nova Southeastern University
Fort Lauderdale, FL 33328
USA

E-mail: kandalam@nova.edu

Received: February 22, 2020
Accepted: July 24, 2020
Online Publication Date: September 18, 2020